Rab25 regulates integrin expression in polarized colonic epithelial cells

Moorthy Krishnan[a], Lynne A. Lapierre[a,b], Byron C. Knowles[a,c], and James R. Goldenring[a,b,c,d]
[a]Section of Surgical Sciences and the Epithelial Biology Center, [c]Department of Cell and Developmental Biology, and [d]Vanderbilt-Ingram Cancer Center, Vanderbilt University Medical Center, Nashville, TN 37232; [b]Nashville Veterans Affairs Medical Center, Nashville, TN 37212

ABSTRACT **Rab25 is a tumor suppressor for colon cancer in humans and mice. To identify elements of intestinal polarity regulated by Rab25, we developed Caco2-BBE cell lines stably expressing short hairpin RNA for Rab25 and lines rescuing Rab25 knockdown with reexpression of rabbit Rab25. Rab25 knockdown decreased α2-, α5-, and β1-integrin expression. We observed colocalization and direct association of Rab25 with α5β1-integrins. Rab25 knockdown also up-regulated claudin-1 expression, increased transepithelial resistance, and increased invasive behavior. Rab25-knockdown cells showed disorganized brush border microvilli with decreases in villin expression. All of these changes were reversed by reintroduction of rabbit Rab25. Rab25 knockdown altered the expression of 29 gene transcripts, including the loss of α5-integrin transcripts. Rab25 loss decreased expression of one transcription factor, ETV4, and overexpression of ETV4 in Rab25-knockdown cells reversed losses of α5β1-integrin. The results suggest that Rab25 controls intestinal cell polarity through the regulation of gene expression.**

Monitoring Editor
Benjamin Margolis
University of Michigan Medical School

Received: Oct 16, 2012
Revised: Dec 20, 2012
Accepted: Jan 16, 2013

INTRODUCTION

Epithelial cells maintain a polarized barrier between the external and internal milieus by assembling discrete apical and basolateral domains separated by tight and adherens junctions (Marrs *et al.*, 1995). The polarized domains in the epithelial cells allow trafficking of critical cell adhesion molecules to apical or basolateral domains and also define regions for elaboration of apical specializations, including brush border microvilli (Mellman and Nelson, 2008). Perturbations of these polarized functions are believed to induce some of the earliest changes that predispose to epithelial-to-mesenchymal transformation (Royer and Lu, 2011). This process of increasing losses in polarity appears to be incremental, such that loss of individual components per se is not able to induce dysplastic changes, but multiple coincident aberrations can lead to the loss of polarized function and disorganization of the epithelial monolayer (Jones *et al.*, 2006). These results all suggest that alterations in membrane protein-trafficking pathways have the potential to lead to deleterious changes in cell polarity.

The successful establishment of polarized epithelial domains is facilitated by discrete intracellular vesicle-trafficking pathways that deliver cargoes to appropriate membrane pathways. These pathways have been delineated in detail in renal Madin–Darby canine kidney (MDCK) cells, for which a number of investigations have demonstrated the separation of membrane recycling pathways for basolateral recycling, apical recycling, and transcytotic pathways between the apical and basolateral membranes (Wang *et al.*, 2000; Lapierre *et al.*, 2001, 2012; Tzaban *et al.*, 2009). The Rab small GTPases and their effectors are critical regulators of these polarized membrane trafficking pathways (Mellman and Nelson, 2008). In addition to mediation of dynamic intracellular trafficking pathways for recycling, Rab proteins are also key mediators of the initiation of

This article was published online ahead of print in MBoC in Press (http://www.molbiolcell.org/cgi/doi/10.1091/mbc.E12-10-0745) on January 23, 2013.

M.K. performed experiments, prepared figures, and cowrote the manuscript; L.A.L. performed experiments and reviewed the manuscript; B.C.K. performed experiments and cowrote the manuscript; J.R.G. designed experiments, prepared figures, and cowrote the manuscript.

None of the authors has any conflict of interest.

Address correspondence to: James R. Goldenring (jim.goldenring@vanderbilt.edu).

Abbreviations used: EGF, epidermal growth factor; ETV4, translocation variant 4; KD, knockdown; RT-PCR, reverse transcription-PCR; shRNA, short hairpin RNA; SI, sucrase Isomaltase; TER, transepithelial resistance.

MDCK cell polarity and the establishment of apical specializations such as primary cilia (Boehlke *et al.*, 2010; Bryant *et al.*, 2010; Roland *et al.*, 2011). Much less is known about trafficking pathways in polarized intestinal epithelial cells. The junctions of polarized intestinal epithelial cells are clearly undergoing continuous remodeling mediated by vesicle trafficking (Shen *et al.*, 2008). In addition, correct trafficking of integrins to appropriate plasma membrane surfaces is required for polarized intestinal epithelial function (Kuwada and Li, 2000). Furthermore, the recent identification of mutations in myosin Vb as the cause of the loss of microvilli in neonates with microvillus inclusion disease has highlighted the importance of membrane trafficking pathways in establishing the components of the apical intestinal brush border (Erickson *et al.*, 2008; Muller *et al.*, 2008).

We previously demonstrated that the epithelial-specific small GTPase Rab25 (Goldenring *et al.*, 1993) is a candidate tumor suppressor in the colon (Nam *et al.*, 2010). Other studies also implicated Rab25 in carcinogenesis in other epithelial cancers (Cheng *et al.*, 2004, 2006, 2010; Vuoriluoto *et al.*, 2011; Dozynkiewicz *et al.*, 2012). Human colon cancers demonstrate a stage-independent reduction in Rab25 expression (Nam *et al.*, 2010). Moreover, whereas Rab25-deficient mice do not manifest a significant intestinal phenotype, the combination of Rab25 knockout with either expression of mutant APC^{Min} or heterozygous loss of Smad3 induces accelerated intestinal neoplasia (Nam *et al.*, 2010). In particular, $Rab25^{-/-}$;$Smad3^{+/-}$ mice develop large, regionally invasive colon cancers. Although these studies established Rab25 as a tumor suppressor in the colon, they could not address the range of cell polarity changes that might account for the induction of neoplasia.

We investigated the molecular mechanisms responsible for the aberrant effects of Rab25 loss in enterocytes through the examination of the knockdown of Rab25 expression in polarized Caco2-BBE cells. Caco2-BBE cells comprise a critical model of intestinal epithelial cells because they polarize and elaborate a mature and well-organized microvillar brush border during 15 d of culture on permeable Transwell filters (Peterson and Mooseker, 1992). We found that short hairpin RNA (shRNA)–mediated knockdown of Rab25 expression in Caco2-BBE cells leads to a loss of α5β1-integrins at the plasma membrane and these changes are reversed by reintroduction of rabbit Rab25. Moreover, loss of Rab25 expression also elicited alterations in claudins, increases in transepithelial resistance, increases in soft agar colony formation, and increases in cell invasion. Rab25 loss also caused alterations in a discrete set of genes, including down-regulation of transcripts for α5-integrin and up-regulation of sucrase isomaltase transcripts. Of importance, Rab25 loss also down-regulated expression of the transcriptional regulator ETV4, and reintroduction of ETV4 into Rab25 knockdown cells led to normalization of α5-integrin and sucrase isomaltase expression. These findings demonstrate that Rab25 regulates intestinal cell polarity through regulation of gene transcription.

RESULTS

Rab25 is up-regulated during polarization in Caco2-BBE cells

Although recent studies suggested that Rab25 is a tumor suppressor in mice and humans for colon cancer (Nam *et al.*, 2010), no previous investigations examined the association of Rab25 with polarity and vesicle trafficking in colonic cell lines. We investigated the expression of Rab25 in eight different colorectal cancer cell lines. Figure 1A demonstrates that all of the cell lines with some capacity to polarize and differentiate expressed Rab25 protein. In contrast, the poorly differentiated SW480 and SW620 lines did not express Rab25. We therefore sought to examine whether Rab25 contributes to intestinal epithelial cell polarity, using the human colonic Caco2-BBE and HCA-7 cell lines, which develop highly polarized monolayers when grown on Transwell filters. In particular, Caco2-BBE cells comprise a unique model for intestinal cell polarity because they develop full polarization expression of resident microvillar structural proteins as well as brush border enzymes (Peterson and Mooseker, 1992). The Caco2-BBE cells were grown on Transwell filters, and the protein expression was analyzed at 3, 8, and 15 d of culture on filters. As previously noted (Peterson and Mooseker, 1992), expression of the brush border proteins villin-1 and sucrase-isomaltase (SI) increased with polarization of Caco2-BBE cells (Figure 1, B and D). Caco2-BBE cells expressed low levels of Rab25 on day 3, with increasing levels of expression during polarization over 15 d on Transwells (Figure 1, C and D). No significant changes were observed in the expression of other Rab proteins, including Rab11a, Rab5, Rab8a, and Rab21 (Supplemental Figure S1A). Because our earlier studies implicated Rab25 in the expression of integrins (Nam *et al.*, 2010), we evaluated integrin expression during polarization. Of interest, as previously noted (Levy *et al.*, 1998), expression of both α2-integrin and β1-integrin was highest at 3 d in culture and decreased during polarization (Figure 1, B and D). In contrast, expression of α5-integrin increased during polarization, similar to the pattern for Rab25 (Figure 1, B and D). We observed a similar increase in Rab25 and α5-integrin expression during polarization in HCA-7 cells; however, levels of α2-integrin and β1-integrin remained stable throughout 15 d of culture on Transwells (Supplemental Figure 1B). These results suggested that increases in Rab25 and α5-integrin expression might be characteristic of colonic cell polarization.

We next sought to evaluate whether changes in Rab25 protein expression were a reflection of changes in gene expression during polarization. The reverse transcription (RT)-PCR and quantitative PCR analysis (Figure 1, E and F) showed that the expression of Rab25 mRNA increased significantly on both 8 and 15 d in culture for Caco2-BBE cells. Thus Rab25 gene and protein expression were both increased during the process of Caco2-BBE cell polarization.

Knockdown of Rab25 alters integrin expression and localization in polarized Caco2-BBE cells

The integrins are heterodimeric transmembrane proteins composed of α and β subunits, which heterodimerize in different combinations. Increasing evidence indicates that alterations in Rab25 regulate integrin expression, especially α5- and β1-integrins, both in vivo and in vitro (Cheng *et al.*, 2004; Caswell *et al.*, 2007; Nam *et al.*, 2010; Lapierre *et al.*, 2011). Therefore we examined the role of Rab25 in the regulation of multiple isoforms of α- and β-integrins at different stages of polarity. We established Caco2-BBE cell lines stably expressing 1) scrambled shRNA (Control), 2) shRNA directed against human Rab25 (Rab25KD), and 3) Rab25KD cells with reintroduction of rabbit Rab25 (Rescue). In Rab25KD cells, Rab25 mRNA (Figure 2A) and protein expression (Figure 2B and Supplemental Figure S2A) were greatly reduced throughout culture for up to 15 d. Rescue with rabbit Rab25 expression did not alter the knockdown of endogenous human Rab25 mRNA in the Caco2-BBE cells (Figure 2A). The expression of Rabbit Rab25 in Rescue cells remained stable throughout 15 d of polarized cell culture (unpublished data). Of note, Rab25 knockdown did not elicit any significant changes in the expression of Rab5, Rab8a, Rab11a, or Rab21 (Supplemental Figure S1C).

We next examined the effects of Rab25 knockdown and rescue on the expression of integrins. As seen in Figure 1B, α5-integrin expression increased with polarity, but Rab25KD cells showed a prominent loss of α5-integrin expression throughout 15 d in culture

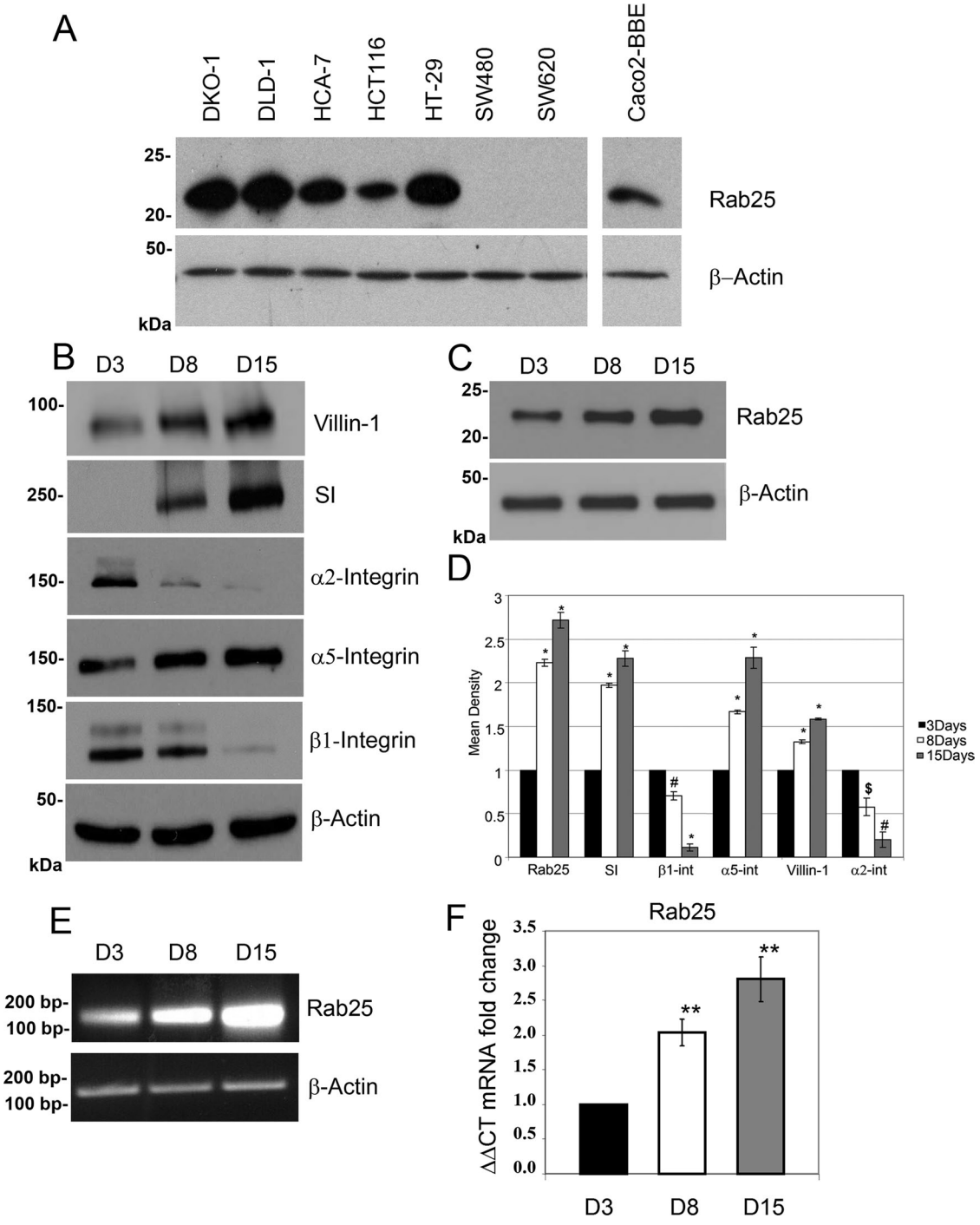

FIGURE 1: Rab25 expression increases with polarity in polarized epithelial cell lines. (A) Endogenous expression of Rab25 in colorectal cancer cell lines. Blots were probed with a polyclonal antibody that was specific for human Rab25. (B) Protein expression for enterocyte differentiation markers villin-1 and SI and integrins β1, α2, and α5 were analyzed in Caco2-BBE cells grown on Transwells for 3, 8, and 15 d. (C) Rab25 protein expression was assessed in protein lysates from Caco2-BBE cells grown on Transwells for 3, 8, and 15 d by immunoblot. (D) Densitometric analysis of protein expression in Caco2-BBE cells. $^{*}p < 0.0001$, $^{\#}p < 0.0005$, and $^{\$}p < 0.01$ compared with protein expression at 3 d. (E) Rab25 mRNA levels were analyzed by RT-PCR in Caco2-BBE cells plated as described. (F) The Rab25 mRNA expression was analyzed by quantitative real-time PCR (normalized to GAPDH) in Caco2-BBE cells in different stages of polarization. Values (fold change) are mean ± SD from three separate experiments. $^{**}p < 0.0005$ compared with mRNA expression at 3 d.

(Figure 2B and Supplemental Figure S2A). Nevertheless, reintroduction of untagged rabbit Rab25 in Rescue cells restored α5-integrin expression to control levels (Figure 2B). It is important to note that we prepared the rescued stable line with untagged Rab25 because we found that expression of mCherry-tagged rabbit Rab25 did not rescue the changes induced by Rab25 knockdown (unpublished data). Whereas α2-integrin expression decreased with polarity in Control cells, Rab25 knockdown elicited further decreases in

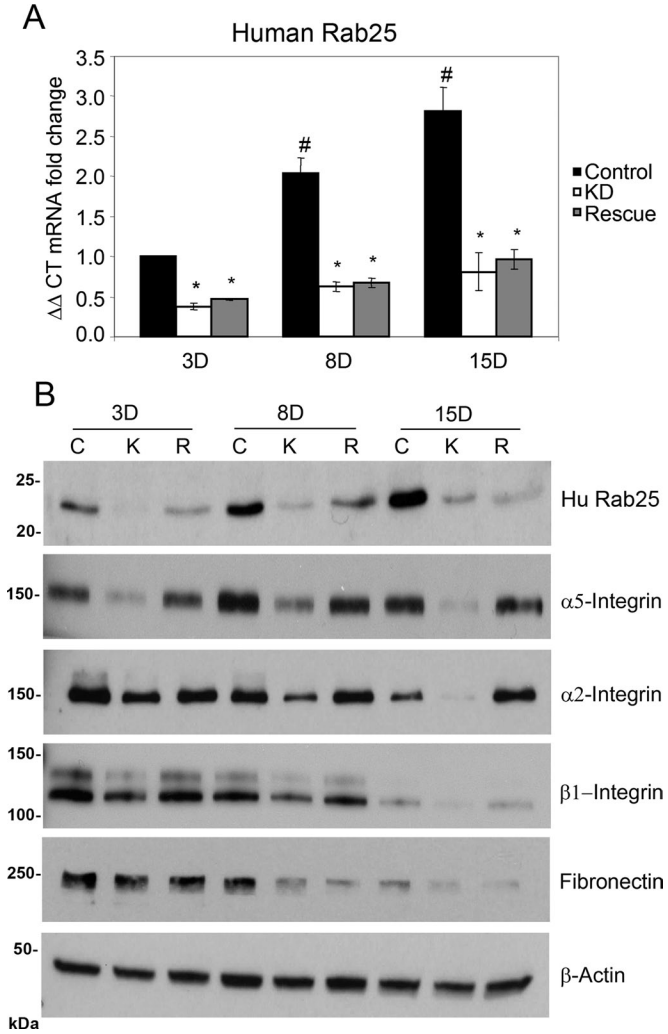

FIGURE 2: Alteration of Rab25 expression alters expression of integrins. Caco2-BBE cell lines were prepared stably expressing scrambled shRNA (Control, C), shRNA targeting human Rab25 (KD, K), and Rab25KD cells stably reexpressing rabbit Rab25 (Rescue, R). Cells were grown on Transwell filters for 3, 8, and 15 d. (A) Quantitative real-time PCR was used to analyze expression of endogenous human Rab25. *$p < 0.001$ compared with days-matched Control, #$p \leq 0.0005$ compared with expression on day 3. Data are representative of three separate experiments. (B) Cell lysates were analyzed for human Rab25 (Hu Rab25), integrins β1, α2, and α5, and fibronectin by immunoblotting. The membrane was reprobed for β-actin as a loading control.

expression. However, in the Rab25 Rescue line, α2-integrin levels were maintained at the levels seen in Control cells (Figure 2B and Supplemental Figure S2B). The maintenance of α2-integrin expression may reflect the stable expression levels for Rab25 throughout the culture period, consistent with expression from pCB6-Rab25. Whereas β1-integrin levels also declined in Control cells during 15 d of polarization on filters, Rab25KD cells showed significant decreases in β1-integrin expression (Figure 2B). The decreases in β1-integrin expression were reversed by reintroduction of rabbit Rab25 in Rescue cells but only to the levels of Control cells at 3, 8, or 15 d in culture (Figure 2B and Supplemental Figure S2B). We also observed a decrease in fibronectin expression during culture of cells on filters, but this was not significantly altered by either knockdown of Rab25 expression or Rescue (Figure 2B and Supplemental Figure S2C).

Because these studies all suggested that loss of Rab25 altered integrin protein expression, we evaluated the distribution of integrins by immunofluorescence microscopy. Unfortunately, no specific antibodies are available to assess α2-integrin expression with immunofluorescence, so we examined the distribution of α5-integrin and β1-integrin. Rab25KD cells showed a decrease in overall α5-integrin expression and a marked decrease in plasma membrane α5-integrin at 3, 8, and 15 d in culture (Figure 3A). These decreases were abrogated in the Rab25 Rescue cells (Figure 3A). No changes were observed for lateral membrane expression of E-cadherin in Rab25KD or Rab25 Rescue cells throughout 15 d in culture (Figure 3B). Similar to the findings for α5-integrin, in Rab25KD cells we also observed losses of β1-integrin expression, especially at the plasma membrane, which were again rescued with reintroduction of rabbit Rab25 (Figure 3C).

Given the changes in integrin expression, we also sought to evaluate the expression of mRNA transcripts for α5-integrin and β1-integrin. Supplemental Figure S3A demonstrates that knockdown of Rab25 elicited decreases in α5-integrin mRNA expression that were significant at 8 and 15 d of polarized culture. Nevertheless, Rab25 Rescue cells showed normal levels of α5-integrin mRNA expression. In contrast, we did not see any decreases in β1-integrin mRNA in the Rab25KD-Caco2-BBE cell lines during 15 d of culture (Supplemental Figure S3B). These studies indicated that Rab25 might influence gene expression in Caco2-BBE cells.

Rab25 regulates integrin localization in Caco2-BBE cells

Caswell *et al*. (2007) demonstrated that overexpressed Rab25 in ovarian cancer cells directly interacts with α5β1-integrin. We therefore sought to examine whether Rab25 associated directly with α5β1-integrin in Caco2-BBE cells. We first compared the distribution of endogenous Rab25 with endogenous Rab11a. We observed only a small overlap of endogenous Rab25-staining vesicles with Rab11a (Figure 4A). The Manders coefficients for colocalization and Pearson's coefficient were higher than those seen for colocalization between the Golgi marker GM130 and Rab25 but still showed only a minor overlap (Figure 4E). A recent investigation in ovarian cells suggested that Rab25 might associate with elements of the late endosomal system (Dozynkiewicz *et al*., 2012). We therefore also examined whether Rab25-containing vesicles were late endosomes. Figure 4B demonstrates that there was little overlap of endogenous Rab25 staining with Rab7 staining and both the Manders coefficients and Pearson's coefficient were generally lower than those seen with Rab11a (Figure 4E), suggesting that the Rab25 vesicles were distinct from Rab7-staining late endosomes. We next examined whether integrins localized with Rab25 on trafficking vesicles. Figure 4, C and D, shows that both α5-integrin and β1-integrin staining was present in Rab25-containing vesicles. High Manders coefficients were seen with both integrins, with >20% of each associated with Rab25-containing vesicles. Finally, we examined whether Rab25 directly interacted with the integrins in Caco2-BBE cells. For these studies, we constructed a second Rescue line stably expressing myc-tagged rabbit Rab25 in Rab25KD cells. Unlike the fluorescent protein chimeras, the smaller myc tag allowed rescue. By immunoisolating myc-Rab25 from rescued cells and evaluating integrin coisolation in Western blots (Figure 4E), we found that both α5-integrin and β1-integrin were coisolated with myc-Rab25. We also determined that immunoprecipitating antibodies against endogenous α5-integrin could coisolate myc-Rab25 (Figure 4F). All of these studies suggest that Rab25-containing vesicles can traffic α5β1-integrins.

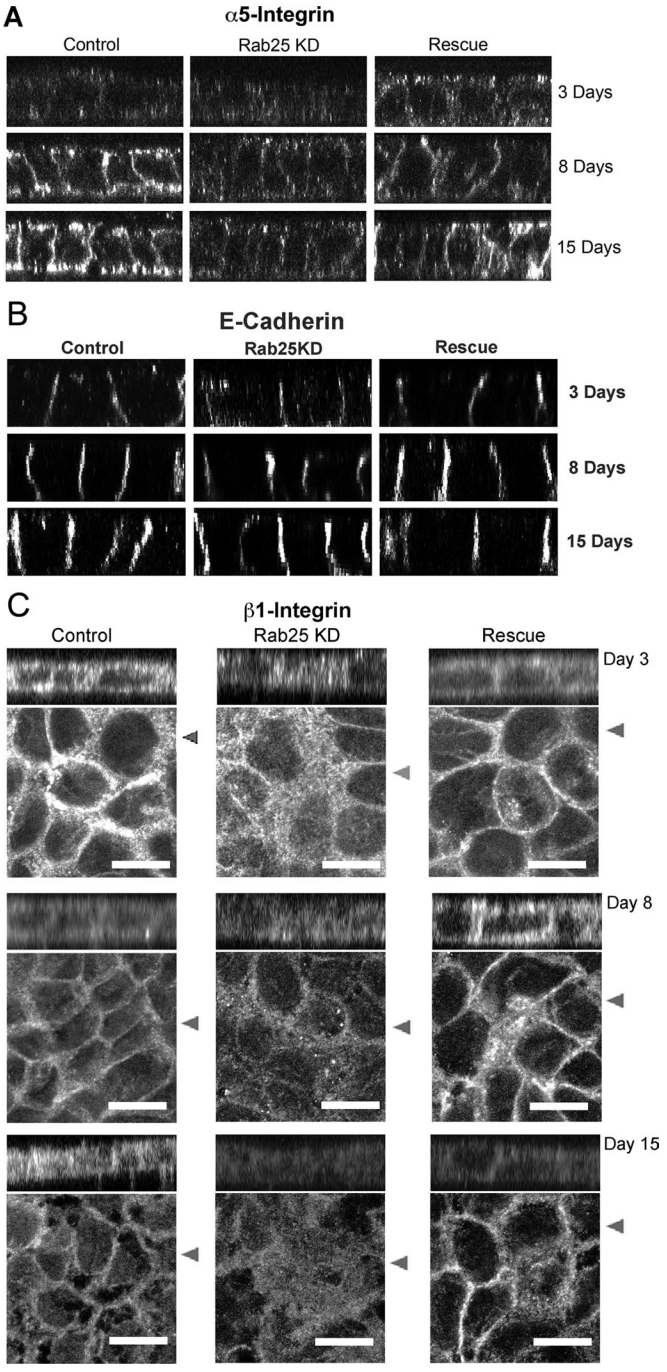

FIGURE 3: Rab25 depletion causes a loss of integrins from Caco2-BBE cells. (A) All three Caco2-BBE cell lines at different stages of polarity were fixed with methanol and stained for α5-integrin. *X-Z* confocal fluorescence images are shown and are representative of at least three experiments. (B) Cells grown as in A were stained for E-cadherin. *X-Z* confocal fluorescence images are shown and are representative of at least three experiments. (C) To test the localization for β1-integrin, Caco2-BBE cells were fixed with paraformaldehyde and stained for human β1-integrin. *X-Z* confocal fluorescence images are shown above single *X-Y* sections. The experiments were repeated at least three times. Bar, 10 μm.

Rab25 alters the development of the brush border

To examine the effects of Rab25 loss on the formation of the apical brush border, we examined Control, Rab25KD, and Rab25 Rescue cell lines cultured for 15 d on Transwell filters by scanning electron microscopy (SEM). Figure 5A demonstrates that, compared with the well-organized brush border observed in Control cells, the Rab25KD cells showed a sparser and more disorganized brush border, with clustering of microvillar groups rather than a tightly packed brush border. Reintroduction of rabbit Rab25 elicited a return of the more organized brush border configuration. Given these findings, we next examined the expression and distribution of the brush border components villin-1 and sucrase isomaltase. By Western blots, villin protein levels were only slightly decreased by Rab25 knockdown at all three days studied (Figure 5B and Supplemental Figure S4A). By immunofluorescence, we did observe a decrease in villin staining in apical region of the cells (Figure 5C). This loss in apical villin was restored with reintroduction of Rab25 in Rescue cells.

In contrast with villin, in Rab25KD cells we observed a surprising up-regulation of sucrase isomaltase expression, especially at 8 and 15 d of culture (Figure 5B and Supplemental Figure S4B). In Rescue cells, sucrase isomaltase levels returned to those observed in Control cells. By immunofluorescence, 15 d cultured cells showed elevated SI staining, which was distributed throughout the cytoplasm. However, there was an apparent absence of SI in the apical membranes (Figure 5D). Reexpression of Rab25 in Rescue cells reestablished a more normal pattern of SI distribution in the apical membranes. As with the integrins, we also evaluated the effects of Rab25 knockdown and Rescue on the expression of SI mRNA transcripts (Figure 5E). Of interest, Rab25 knockdown elicited a marked elevation of SI transcript expression that returned to control levels in cells rescued with rabbit Rab25 (Figure 5E). The results indicate that Rab25 regulates both assembly of the brush border and gene transcription of brush border components.

Rab25 depletion alters claudin expression

Tight junctions provide a continuous intercellular seal, mediate paracellular transport, act as fence between apical and basolateral membranes, and regulate cell polarity (Shen *et al.*, 2008). Because depletion of Rab25 caused perturbation of the apical membrane specializations, we evaluated whether loss of Rab25 affected tight junction proteins and their function. We first measured the transepithelial resistance (TER) in all three cell lines from day 3 to day 15 (Figure 6A). The TER values increased from day 3 to day 15 in all three cell lines. However, compared with Control cells, we observed a prominent increase in TER in Rab25 KD cells after 8 d in culture. Rescue cells with rabbit Rab25 expression showed lower TER than Controls throughout the 15 d in culture (Figure 6A).

The alterations in TER suggested that Rab25 might regulate tight junction components. We therefore analyzed tight junction proteins by Western blots (Figure 6B and Supplemental Figure S4, C and D). Similar to previous findings (Buzza *et al.*, 2010), the Control Caco2-BBE cells expressed low levels of claudin-1 in less polarized cells (day 3), with increasing amounts observed at 8 and 15 d in culture (Figure 6B and Supplemental Figure S4C). In contrast, we observed a decrease in the expression of claudin-2 in Control cells during the 15 d in culture. In the Rab25KD cells, we observed a prominent increase in claudin-1 expression. Overall, levels of claudin-2 expression during polarizing cell culture showed little significant change except at 15 d (Supplemental Figure S4C). In Rab25 Rescue cells, we found a decrease of claudin-1 expression toward control levels (Figure 6B and Supplemental Figure S4C). In addition, we also examined the expression of claudin-3, -4, and -7. Expression of claudin-3 and claudin-4 was stable throughout the 15 d in culture in Control cells. Rab25KD cells showed small, consistent decreases in the expression of claudin-3 and claudin-4 that were reversed in the Rab25 Rescue cells (Figure 6B and Supplemental Figure S4C).

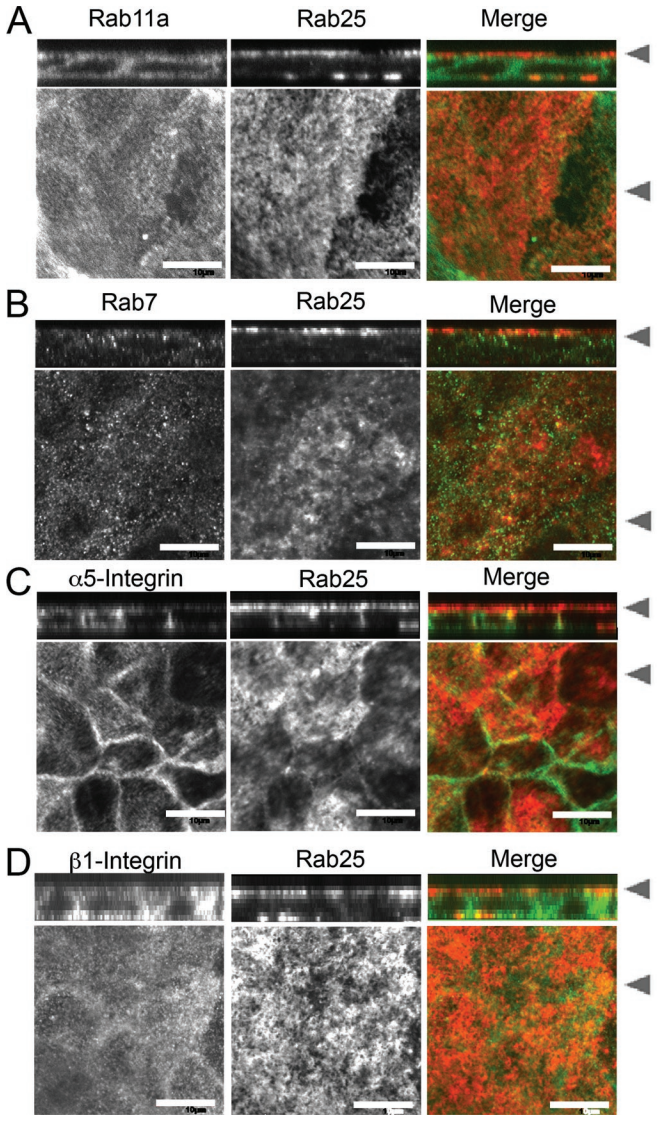

E

	Protein colocalized with Rab25 (Mander's coefficient)	Rab25 colocalized with Protein (Mander's coefficient)	Pearson coefficient (r)
Rab11a	0.1168	0.0883	0.0716
α5-Integrin	0.2465	0.0684	0.1854
β1-Integrin	0.2013	0.0750	0.3099
Rab7	0.0737	0.0984	0.0492
GM130	0.0185	0.0302	0.0326

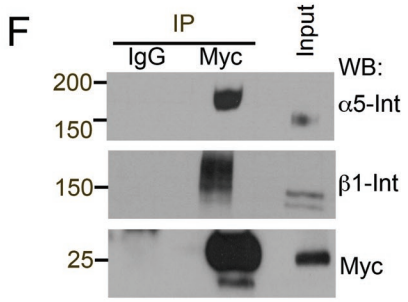

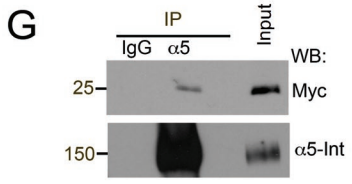

FIGURE 4: Rab25 associates with α5β1-integrin in Caco2-BBE cells. (A) Caco2-BBE cells were grown on Transwells and stained for endogenous expression of Rab25 and Rab11a. For the colocalization of Rab25 with (B) Rab7, (C) α5-integrin, and (D) β1-integrin, the BBE cells were grown on Transwells for 8 d, fixed with 4% paraformaldehyde, and stained using a TSA Kit. Bars, 10 μm. (E) Colocalization between Rab25 and other immunostains was determined, and the Manders comparison coefficients and Pearson coefficient were calculated. (F) Rab25KD cells stably transfected with myc-rabbit Rab25 were grown on Transwell filters for 5 d in culture and lysed with 1% CHAPS buffer, and immunoprecipitations were performed with anti-myc or nonspecific IgG; immunoisolates were probed on Western blots for α5-integrin, β1-integrin, and myc. Input staining at right was for 20% of the lysate used in the immunoprecipitations. (G) Cells were lysed as in F, and immunoprecipitations were performed with anti–human α5-integrin or nonspecific IgG; immunoisolations were analyzed in Western blots for myc and α5-integrin. Input staining at right was for 20% of the lysate used in the immunoprecipitations. Results are representative of three separate experiments.

Claudin-7 expression increased during the 15 d in culture for all three cell lines, but expression was not affected by loss of Rab25 expression (Supplemental Figure S4D). We also did not observe any changes in the expression of either ZO-1 or occludin in any of the cell lines throughout the 15 d in polarizing culture (Supplemental Figure S4D).

We next evaluated the distribution of claudins using immunostaining (Supplemental Figures S5–S8). These studies confirmed that Rab25KD caused an increase in claudin-1 staining, with more prominent extension of claudin-1 along the lateral membrane compared with Control or Rescue cells (Supplemental Figure S5). In contrast, in Rab25KD cells, we observed prominent decreases in the staining of tight junctions for claudin-2, claudin-3, and claudin-4 (Supplemental Figures S6–S8). Overall, these studies suggest that alterations in the ratios between claudin-1 and claudin-2 expression could account for the differences in TER observed in Rab25KD cells.

Rab25KD cells show increased colony formation and cell invasion

Because alterations in integrins and tight junction proteins can lead to changes in cancer cell invasion, we examined these properties in the Control, Rab25KD, and Rescue cell lines. In soft agar colony formation assays, we observed a twofold increase in the number of colonies formed and a significant increase in colony size in Rab25KD

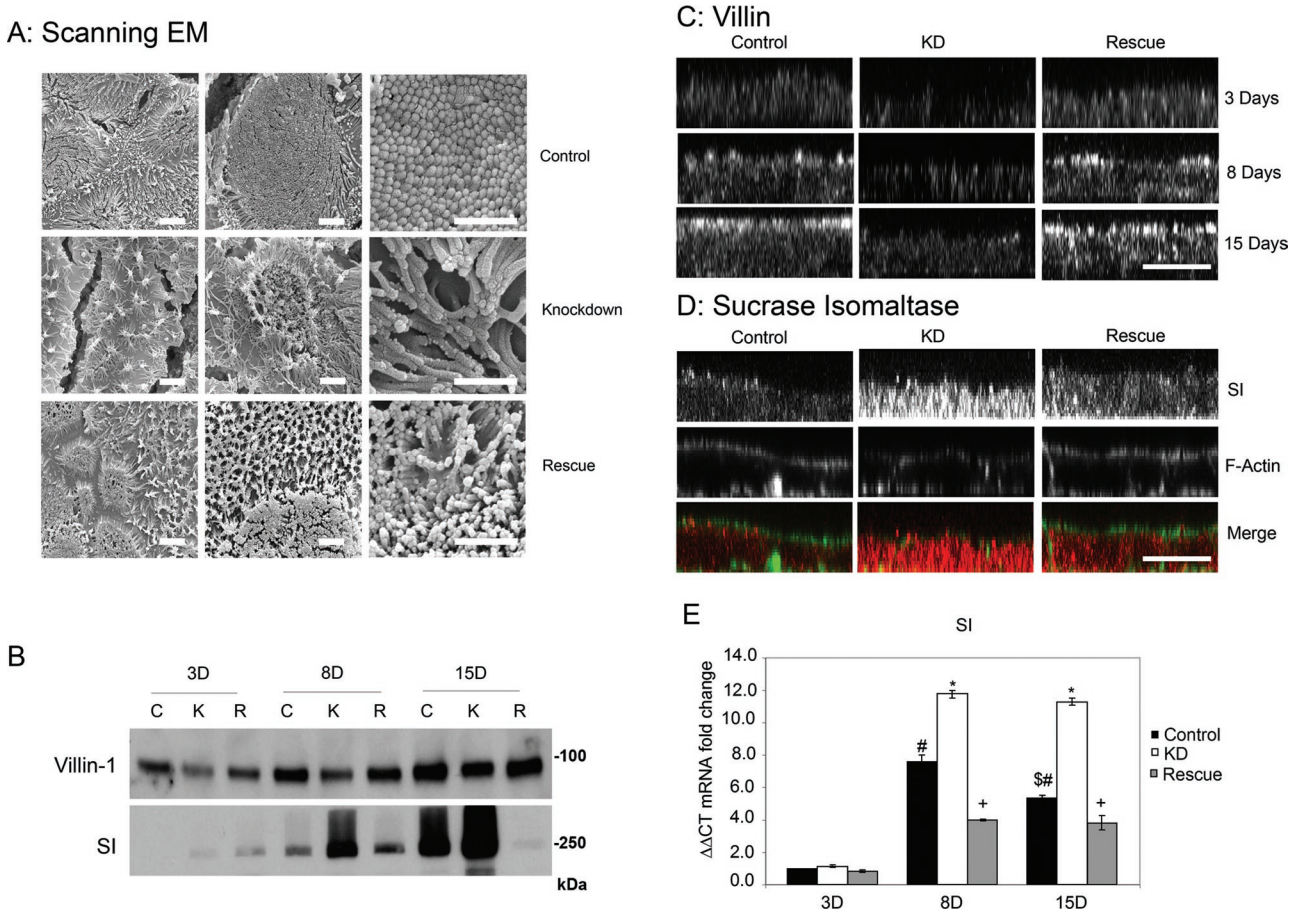

FIGURE 5: Rab25 loss alters the Caco2-BBE apical brush border. (A) Scanning electron microscopy was used to visualize the apical brush border in Control, Rab25KD, and Rab25 Rescue cells. Cells were grown on Transwell filters for 15 d and fixed with 3% glutaraldehyde in SEM buffer. Bar, 10 μm (left and middle), 1 μm (right). (B) Protein expression of villin-1 and the apical membrane-anchored hydrolase SI were analyzed in total cell lysates by Western blot at different stages of polarity in Control, Rab25KD, and Rescue cells. (C) The three cell lines were fixed with 4% PFA on the indicated days and stained for villin-1. *X-Z* confocal fluorescence images shown are representative of three separate experiments. Bar, 10 μm. (D) Control, Rab25KD, and Rescue Caco2-BBE cells were grown for 15 d on Transwell filters, fixed with 4% PFA, and stained for SI (red in merge) and F-actin (green in merge). *X-Z* confocal fluorescence images shown are representative of three separate experiments. Bar, 10 μm. (E) RNA was isolated from all three cell lines, and SI mRNA expression was analyzed by quantitative RT-PCR. The data are from at least three separate experiments and are presented as the mean ± SD. $^{\#}p < 0.001$ compared with 3-d control value, $^{\$}p \leq 0.05$ compared with 8-d control value, $^{*}p < 0.0001$ compared with days-matched control, and $^{+}p < 0.001$ compared with Rab25KD.

cells compared with Control cells (Figure 7A). Reintroduction of rabbit Rab25 in Rescue cells reversed the effects of Rab25 knockdown. In general, Caco2-BBE cells show slow migration in cell invasion assays. We studied cell-invasive capacity using an xCELLigence system (Roche) for continuous monitoring of the cell migration (Figure 7B). We did not observe any migration until ~25 h in culture, after which we observed an acceleration in migration by Rab25KD cells that was not observed in either Control or Rescue cell lines. These findings indicate that loss of Rab25 can promote invasive characteristics in Caco2-BBE cells.

Modulation of Rab25 alters the gene expression

Because our investigations suggested that loss of Rab25 was associated with decreases in α5-integrin mRNA expression, we performed gene microarray analysis of mRNA transcripts in Control, Rab25KD, and Rescue Caco2-BBE cell lines. We sought to identify transcripts whose expression was either significantly increased or decreased in Rab25KD cells and then restored to control levels in Rescued cells. We identified only 29 genes with greater-than-fourfold changes between Control and Rab25KD that were normalized in the Rescue cell line (Table 1). Twenty-two transcripts were up-regulated with loss of Rab25, and seven transcripts were down-regulated. Among these transcripts, as seen by quantitative PCR, α5-integrin was down-regulated and SI was up-regulated. Pathway analyses suggested that most of the genes altered by Rab25 knockdown were related to either glucose metabolism or retinoic acid pathways.

Although these findings suggested that Rab25 loss could effect significant changes in gene transcription, we found no evidence, by either isolation of nuclei or immunofluorescence staining, that Rab25 traverses into the nucleus in Caco2-BBE cells (unpublished data). Among the 29 genes, we identified only one transcription factor: ETS translocation variant 4 (ETV4, also known as E1AF or PEA3). We examined the expression of ETV4 during polarization of Caco2-BBE

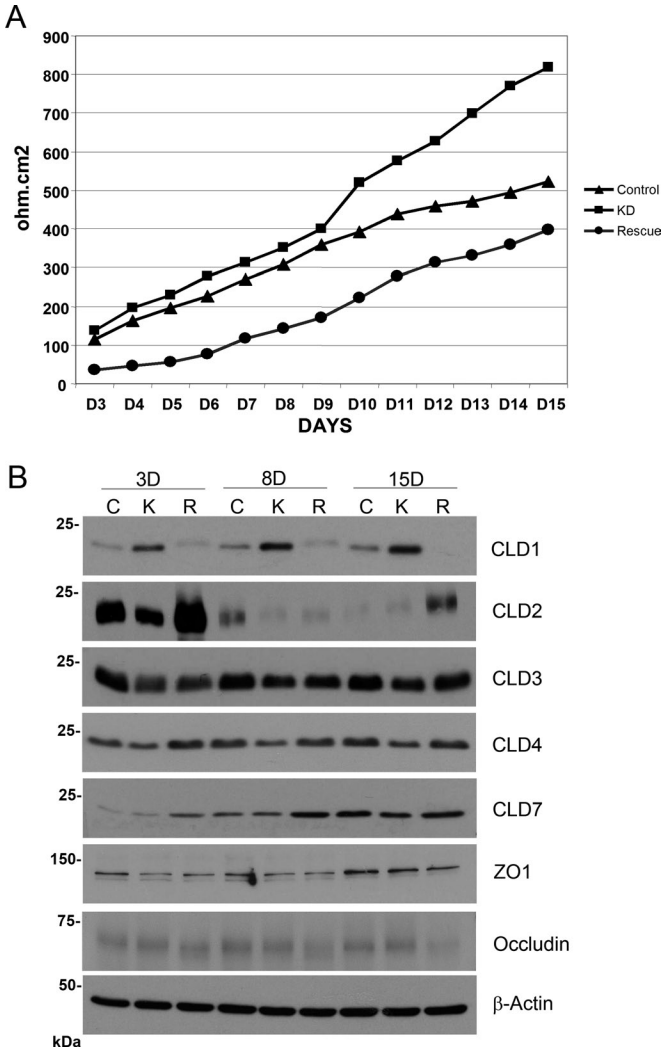

FIGURE 6: Rab25 depletion alters the transepithelial resistance and claudin expression. (A) TER was measured in all cell lines from day 3 to day 15 on Transwell filters. During this period, the media were changed every day, and TER was measured in 24-well Transwell inserts. Results are expressed in ohm-cm^2 and are representative of three separate experiments. (B) Equal amounts of total protein lysates (20 μg) from Control, Rab25KD, and Rescue cells were analyzed by Western blots for tight junction proteins. The blots were subsequently stripped and reprobed for β-actin as a loading control. The results are representative of three separate experiments.

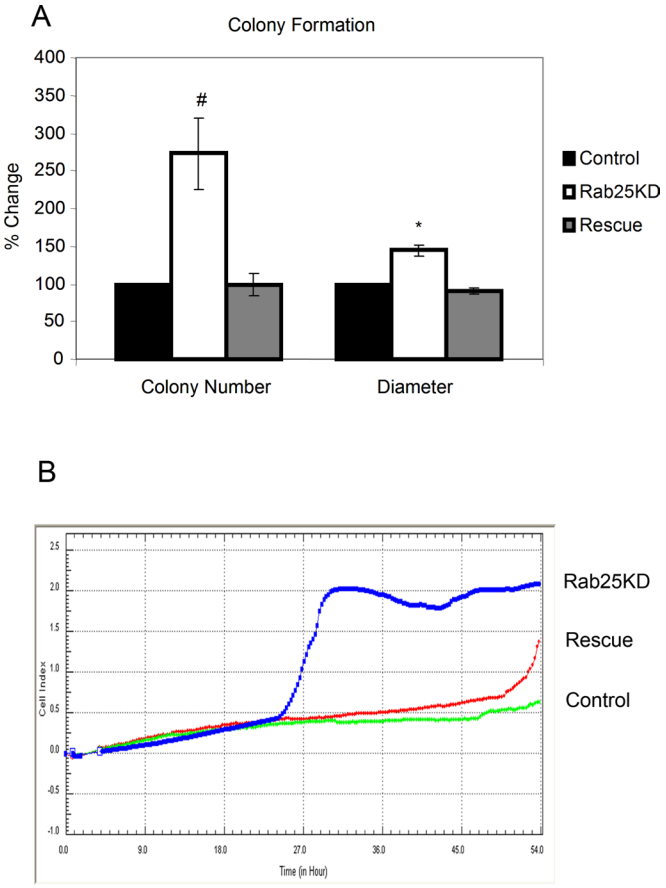

FIGURE 7: Rab25 loss promotes soft agar colony formation and increases the cell migration in Caco2-BBE cells. (A) Control, Rab25KD, and Rescue cell lines were mixed with 0.6% low-melting agarose in DMEM media. Cells were allowed to grow for 21 d. After 21 d, colonies were counted using a GelCount colony counter. Rab25KD cells showed significant increases in the number, as well as in the diameter, of colonies compared with Control and Rescue cells. *$p \leq 0.005$ compared with number of colony formed in control, and #$p \leq 0.0001$ compared with size of the colony formed in control. (B) The three Caco2-BBE cell lines were plated in the top chambers of xCELLigence CIM Plates with serum-free media and serum-containing media and loaded into the lower chamber. The cells were incubated in the RTCA DP Analyzer inside the incubator and measurements were taken every 15 min for 55 h. The representative traces from one experiment show that Rab25KD cells showed increased migration after 24 h, whereas Control and Rescue cells showed more indolent migration throughout. The experiments were performed in triplicate.

cells. No antibodies are available against ETV4 for immunoblot analysis, so we evaluated ETV4 expression by IF. Of interest, the expression of ETV4 immunostaining (Supplemental Figure S9) decreased with polarity. By immunostaining, Rab25 KD cells had lower expression of ETV4 in the nucleus. Rescue of Rab25 elicited an increase in nuclear ETV4 staining (Supplemental Figure S9). We therefore examined whether ETV4 could be the downstream target of the loss of Rab25 by overexpressing mCherry-ETV4 in Rab25 KD cells (Figure 8) and evaluating rescue of the Rab25KD phenotype. Overexpression of ETV4 caused a reduction of SI protein and an increase in α5- and β1-integrins expression similar to that observed in cells rescued with either untagged or Myc-tagged rabbit Rab25 (Figure 8). These results suggest that Rab25 controls gene transcription of these critical polarity proteins through the regulation of ETV4 expression.

DISCUSSION

A number of investigations over the past decade have led to the concept that a loss of polarity is a central driver in the early stages of carcinogenesis. These changes at cellular junctions can involve the mistrafficking of adhesion molecules such as integrins or junctional components such as claudins or alterations in the assembly of proteins such as catenins. All of these scenarios lead to losses in polarized function that individually do not induce phenotypic transformation. Instead, it appears that multiple deficits must be present to induce frank carcinogenesis. Previous studies demonstrated that Rab25 loss, in combination with other alterations in cell behavior, can lead to accelerated tumor formation in the intestine and colon (Nam *et al.*, 2010). The results detailed in the present studies indicate that Rab25 loss not only can alter trafficking pathways for integrins

Probe	Fold change	Gene	GenBank	Gene description
8091811	4.66	SI	BC132834	Sucrase isomaltase
8007429	3.41	G6PC	U01120	Glucose-6-phosphatase, catalytic subunit
8162884	3.01	ALDOB	AK290795	Aldolase B, fructose-bisphosphate
8103326	2.97	FGG	BC007044	Fibrinogen γ chain
8017766	2.90	APOH	BC026283	Apolipoprotein H
8095646	2.80	AFP	BC027881	α-Fetoprotein
8008172	2.64	B4GALNT2	BC113675	β-1,4-*N*-Acetyl-galactosaminyl transferase 2
8020795	2.43	TTR	D00096	Transthyretin
8127072	2.39	GSTA1	BC053578	Glutathione *S*-transferase α1
8100758	2.38	UGT2B7	J05428	UDP glucuronosyltransferase 2 family, polypeptide B7
8097910	2.33	FGB	BC107766	Fibrinogen β chain
8160670	2.24	AQP3	AK095363	Aquaporin 3
7932326	2.22	CUBN	AF034611	Cubilin
8162502	2.18	FBP1	BC012927	Fructose-1,6-bisphosphatase 1
8103311	2.16	FGA	M58569	Fibrinogen α chain
7909441	2.15	G0S2	BC009694	G0/g1switch 2
7940341	2.08	MS4A10	BC137259	Membrane-spanning 4-domains, subfamily A, member 10
8178115	2.08	CFBlC2	BC004143	Complement factor B
7936871	2.07	OAT	BC016928	Ornithine aminotransferase
7945158	2.03	—	—	U6 spliceosomal RNA
8118345	2.01	CFBlC2	BC004143	Complement factor B
7935116	2.00	RBP4	BC020633	Retinol-binding protein 4, plasma
8059852	–2.00	MSL3L2	AK301707	Male-specific lethal 3-like 2
7909568	–2.03	DTL	AK292343	Denticleless homologue
7921099	–2.04	CRABP2	BC001109	Cellular retinoic acid–binding protein 2
8095744	–2.09	AREG	BC009799	Amphiregulin
8015806	–2.19	ETV4	BC016623	ETS variant 4
7963786	–2.49	ITGA5	BC008786	Integrin, α5 (fibronectin receptor, α polypeptide)
8048205	–3.09	IGFBP2	BC004312	Insulin-like growth factor–binding protein 2, 36 kDa

Control, Rab25KD, and Rescue Caco2-BBE cell lines were grown on six-well Transwells for 8 d. Total RNA was isolated using TRIzol and treated with RNase-free DNase. The replicate total RNA samples from separate experiments were submitted for gene expression analysis by Affymetrix microarrays. Gene transcripts were identified with greater-than-fourfold changes between Control and Rab25KD cells that were reversed in the rabbit Rab25 Rescue cells.

TABLE 1: Rab25-regulated gene transcripts.

and claudins, but can also influence gene expression of a discrete set of transcripts relevant to the maintenance of polarity.

The loss of aspects of cellular polarity is a major determinant of cell behavior. Previous studies (Bretscher, 1992; Roberts *et al.*, 2001; Pellinen *et al.*, 2006) showed that most of the integrins are internalized from the membrane into recycling compartments and recycled back to cell surface using small GTPases. Other studies (Cheng *et al.*, 2004; Caswell *et al.*, 2007) implicated Rab25 as a tumor promoter in ovarian cancer cells, in which increases in Rab25 expression cause changes in α5β1-integrins. In contrast, we observed that membrane localization of β1-integrin in enterocytes is disrupted in Rab25-knockout mice (Nam *et al.*, 2010). Previous studies also showed that loss of β1-integrin in the intestinal enterocytes promotes intestinal tumor formation in the mouse and knockdown of β1-integrin expression in Caco2 cells leads to increased invasive properties (Kuwada and Li, 2000). The overexpression of α5β1-integrin in HT29 colon carcinoma cells dramatically reduced tumorigenicity (Varner *et al.*, 1995). Although the different tumor suppressor and tumor promoter activities of Rab25 are not clear, Norman and colleagues suggested that when CLIC3 is expressed, Rab25 is a tumor promoter, whereas it acts as a tumor suppressor in cells lacking CLIC3 expression (Dozynkiewicz *et al.*, 2012). Indeed, we found only low levels of CLIC3 expressed in Caco2-BBE cells (unpublished data). Nevertheless, in both ovarian and intestinal systems, there appears to be consistent data that Rab25 can associate directly with α5β1-integrin. Caswell *et al.* (2007) found evidence for a direct association of overexpressed Rab25 in ovarian cells. In our present investigations, we also observed an association of Rab25 with α5β1-integrins in Caco2-BBE cells. These results suggest that Rab25 mediates context-dependent trafficking decisions that

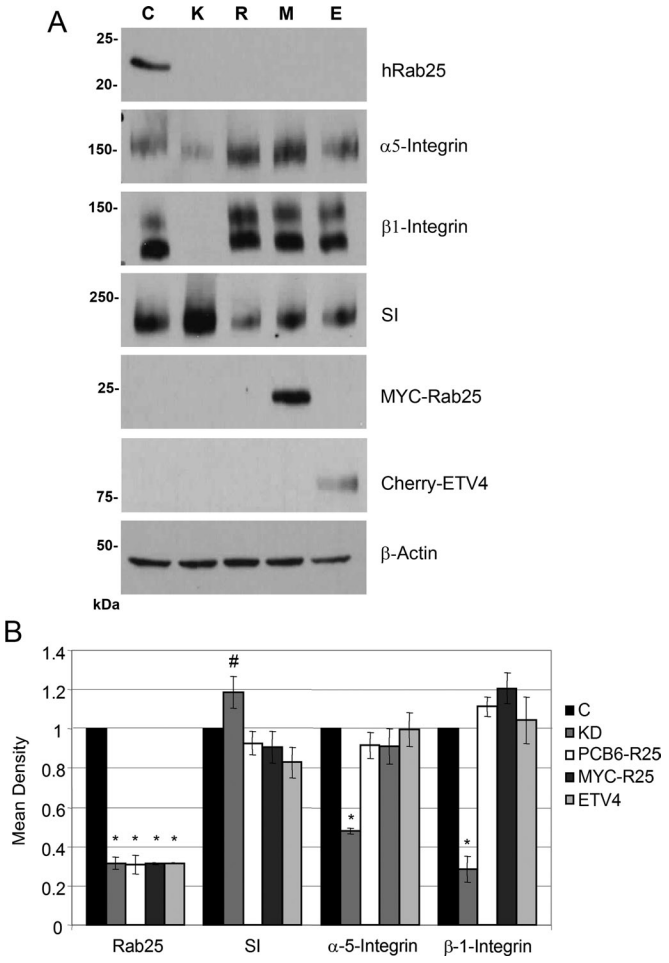

FIGURE 8: Rab25 regulates protein expression through expression of the transcription factor ETV4. (A) Control, Rab25KD, and Rab25KD cells rescued with either untagged rabbit Rab25 (R) or myc-tagged rabbit Rab25 (M) were plated on six-well Transwells. For ETV4 expression, the Rab25KD cells were transiently transfected with mCherry-ETV4 (E). After 8 d in culture, the cells were lysed with RIPA and analyzed by Western blot for endogenous human Rab25, β1-integrin, α5-integrin, and SI. The membrane was reprobed for myc and mCherry to demonstrate expression of the myc-Rab25 and mCherry-ETV4, respectively. (B) Quantitative analysis of three separate experiments. $^{*}p < 0.001$, $^{\#}p < 0.05$ compared with control value.

manifest in cell-specific decisions in cargo presentation at epithelial cell surfaces.

Of importance, whereas both Rab11a and Rab11-FIP1C/RCP were implicated in the regulation of α5β1-integrin trafficking (Caswell and Norman, 2006; Caswell *et al.*, 2007; Lobert *et al.*, 2010), Rab25 loss did not influence the expression or distribution of either Rab11a or Rab11-FIP1C/RCP (unpublished data). Previous studies in breast cancer cells demonstrated that α2β1 recycling is mediated by Rab21 (Pellinen *et al.*, 2006, 2008). We did not observe any change in Rab21 in the Rab25 KD cell line. We also observed reductions in the expression of α2-integrin in Rab25KD Caco2-BBE cells. All of these findings support a complex and dynamic relationship of targeted trafficking events in polarized epithelial cells.

Recent investigations demonstrated that elements of the recycling system regulate the protein composition of the adherens and tight junctions. In MDCK cells, expression of a mutant of Rab11-FIP2 with a serine-to-glutamate mutation that mimics phosphorylation by MARK2/Parlb causes a loss of both E-cadherin from adherens junctions and occludin from tight junctions (Lapierre *et al.*, 2012). Of interest, the cells expressing the S227E mutation do not display any changes in transepithelial resistance, in part because they show an increase in claudin-1 and a decrease in claudin-2 expression. In the present studies, we did not observe significant alterations in adherens junction proteins with loss of Rab25, but we did find an increase in the expression of claudin-1 compared with a prominent decrease in the expression of claudin-2 and to a lesser extent decreases in claudin-3 and -4 in Rab25-knockdown cells. However, we did not observe localization of claudins in Rab25-containing vesicles, so it is not clear how vesicle-trafficking pathways are involved in these changes in junctional properties. The increased expression of claudin-1, as well as the decreased expression of claudin-2, is expected to lead to a decrease in monolayer permeability through the formation of cation-selective ion channels at the tight junctions with particular affinity for the sodium ions and a resultant increase in transepithelial resistance (Hou *et al.*, 2006; Van Itallie and Anderson, 2006). Thus Rab25KD Caco2-BBE cells also demonstrated increased transepithelial resistance. In addition, Rab25KD Caco2-BBE cells also displayed increased soft agar colony formation and invasive cell behavior. Although these properties might seem counterintuitive, previous investigations noted that, as observed for Rab25 loss (Nam *et al.*, 2010), increases in claudin-1 expression were noted previously in human colon cancers independent of tumor stage (Shiou *et al.*, 2007; Krishnan *et al.*, 2010). Thus alterations in barrier junctions, combined with changes in integrins, may lead to invasive properties due to changes in the distribution and function of junctional components. In this case, tighter junctional associations of cells during invasion may lead to a more efficient cell invasion front.

In addition to direct interactions of Rab25 with α5β1-integrins that would be expected to influence trafficking, we also observed a prominent influence of Rab25 on the expression of α5-integrin mRNA transcripts. Rab25 did not influence the mRNA expression of β1-integrin but did lead to a decrease in total β1-integrin protein expression and loss of β1-integrin protein expression at plasma membrane surfaces, similar to that observed in Rab25-deficient mice (Nam *et al.*, 2010). We also found that β1-integrin protein expression decreased with the assumption of mature polarity (Schreider *et al.*, 2002), whereas α5-integrin and Rab25 protein expression increased during maturation of the polarized monolayer. These results suggest that alterations in β1-integrin might be secondary to the major regulation of α5-integrin gene expression as the primary focus for the influence of Rab25 in intestinal cells. No such mechanism has been observed in other systems, such as ovarian cancer, that manifest nonpolarized epithelial phenotypes.

Previously, Rab proteins were not associated strongly with changes in gene regulation. A recent report noted an increase in a number of metabolic genes in association with overexpression of Rab25 in ovarian cancer cells (Cheng *et al.*, 2012). Little if any evidence exists for translocation of Rab small GTPases to the nucleus. Indeed, we have not been able to find any evidence for Rab25 relocation to the nucleus in Caco2-BBE cells (unpublished data). Nevertheless, our findings do indicate that loss of Rab25 leads to discrete changes in gene expression. Loss of Rab25 leads to both up-regulation and down-regulation of genes involved in polarity. The most prominent of these changes are the loss of transcripts for α5-integrin and the marked up-regulation of transcripts for SI. Loss of Rab25 causes the down-regulation of the expression of the transcriptional

regulator ETV4. Reexpression of ETV4 reestablishes the normal expression of both α5-integrin and sucrase isomaltase. It therefore appears that a regulatory cascade exists for control of ETV4 expression that is influenced by Rab25, and transcription of ETV4 mRNA is an intermediary regulator of polarity in enterocytes. Although the results with ETV4 expression in Caco2-BBE cells suggest a tumor suppressor role for ETV4, previous studies suggested that ETV4 is up-regulated in invasive colon cancer (Jung *et al.*, 2011). Nevertheless, other studies identified ETV4 as a key regulator of epithelial cell organization during development (Kuure *et al.*, 2010). Thus, as is the case with other critical regulators, such as the epidermal growth factor (EGF) receptor, expression of ETV4 in the context of the differentiated intestinal phenotype may promote polarity, whereas expression in the context of a dedifferentiated neoplastic phenotype may promote invasive properties.

In summary, the present investigations demonstrate that Rab25 regulates intestinal epithelial cell polarity through alterations in integrin gene expression. At present, it is not possible to pinpoint the connection between Rab25 and the regulation of ETV4 transcription. Further studies will be required to identify transcriptional regulators that might associate with Rab25-containing trafficking membranes. One would assume that sequestration of these factors in the cytoplasm with Rab25-containing vesicles might account for ETV4 transcriptional modulation in a manner similar to that observed for regulators such as β-catenin. Nevertheless, these studies do demonstrate that vesicular trafficking proteins can both directly influence the localization of critical regulators of polarity and affect polarity through the modulation of the cellular transcriptional profile.

MATERIALS AND METHODS

Cell culture and reagents

Caco2-BBE cells were a gift from Matthew J. Tyska (Vanderbilt University, Nashville, TN). Cell culture dishes and Transwells were purchased from Costar (Cambridge, MA). The human colon cancer Caco2-BBE and HCA-7 cell lines and HEK293T cells were grown in DMEM media with 10% heat-inactivated fetal bovine serum and 1% glutamine and penicillin/streptomycin. The cells were cultured on Transwell polycarbonate filters for all the experiments, and media were changed every day throughout the culture duration. The following antibodies were used in this study: Rab25 for Western blot (WB; 1:1000; R4405; Sigma-Aldrich, St. Louis, MO) or affinity-purified rabbit anti-Rab25 (1:100; Nam *et al.*, 2010) and murine monoclonal anti-Rab25 12C3 for immunofluorescence (IF; 1:50; Goldenring *et al.*, 1993); α5-integrin for WB (1:2000; 610633; BD Biosciences, San Diego, CA) and for IF (1:100; 555651; BD Biosciences); α2-integrin for WB (1:500; 611016; BD Biosciences); β1-integrin for WB (1:1000; 610467; BD Biosciences) and for IF (1:50; MAB1959; Millipore Billerica, MA); fibronectin for WB (1:1000; 610077; BD Biosciences); β-actin for WB (1:5000; A5316; Sigma-Aldrich); SI for WB (1:500; HPA011897; Sigma-Aldrich) and rabbit anti-SI for IF (1:100; a gift from Matthew J. Tyska); villin-1 for both WB and IF (1:1000/1:50; 2369; Cell Signaling, Beverly, MA); claudin-1 for both WB and IF (1:2000/1:200; 51-9000; Invitrogen, Carlsbad, CA); claudin-2 for both WB and IF (1:1000/1:100; 51-600; Invitrogen); claudin-3 for both WB and IF (1:1000/1:100; 34-1700; Invitrogen); claudin-4 for both WB and IF (1:2000/1:200; 32-9400; Invitrogen); claudin-7 for WB (1:500; 37-4800; Invitrogen); ZO-1 for WB (1:500; 61-7300; Invitrogen); occludin for WB (1:1000; 71-1500; Invitrogen); DsRed for WB (1:250; 632496; Clontech, Mountain View, CA); rabbit anti-Rab11a for both WB and IF (1:2000/1:200; Ducharme *et al.*, 2006); Rab5 for WB (1:2500; 3547; Cell Signaling); Rab21 for WB (1:2000; R4405; Sigma-Aldrich); Rab7 for IF (1:200; Ab50533; Abcam, Cambridge, MA); Myc-Tag for WB and immunoprecipitation (1:3000/1:50; Vanderbilt Antibody and Protein Resource; VAPR9E10); and affinity-purified rabbit anti-Rab8a for WB (1:3000; Roland *et al.*, 2007). The secondary antibodies (Cy3, Cy5, and horseradish peroxidase conjugated) were obtained from Jackson ImmunoResearch Laboratories (West Grove, PA). Agar was from Lonza (Rockland, ME) and High Capacity cDNA Reverse Transcription Kits were purchased from Applied Biosystems (Foster City, CA).

Rab25 knockdown and DNA constructs

The lentiviral vectors for shRNA targeting human Rab25 and scrambled control shRNA were purchased from Open Biosystems (Lafayette, CO). The shRNA against Rab25 and control shRNA were transfected in HEK293T cells along with packaging vector (pR8.2) and ENV plasmid (pMDG.2) using Effectene reagent (Qiagen, Valencia, CA). The next day the HEK cells were washed and refed with the same media used for the Caco2-BBE cells. After another 48 h the cell supernatant was collected and filtered through a 0.45 μM filter. Caco2-BBE cells were infected with 50% lentiviral-containing media and 50% fresh media with polybrine (5 mg/ml). The cells were stably selected (after 72–96 h of infection) using puromycin (2 μg/ml), and stable cell lines were maintained with 1 μg/ml puromycin. The Rab25 knockdown was confirmed by immunoblotting using anti–human Rab25 antibodies. The cells stably expressing rabbit Rab25 were established by transfection of pCB6-rabbit Rab25 (Casanova *et al.*, 1999) into Rab25-knockdown cells, and clones were selected with 200 μg/ml G418 and 1 μg/ml puromycin. The rabbit Rab25 sequenced was recloned into pMYC-C2 vector between *Eco*RI and *Sal*I. This myc-tagged rabbit Rab25 expression vector was then used to establish stable rescue lines by transfection into Rab25-knockdown cells and G418 selection as described.

Immunoblot

The Caco2-BBE-Control, Rab25KD, and Rescue (both untagged rabbit Rab25 and myc–rabbit Rab25) cells were plated on six-well Transwells for 3, 8, and 15 d and then washed with phosphate-buffered saline (PBS) and lysed in RIPA buffer (50 mM Tris-Cl, pH 7.4, 150 mM NaCl, 1% NP-40, 0.5% sodium deoxycholate, 0.1% SDS) for 10 min at 4°C. The lysate was sonicated for 25 s and centrifuged at 16,000 × *g* for 10 min. The supernatant was transferred to a new tube, and protein concentration was determined by bicinchoninic acid (BCA) method using the Pierce BCA protein assay reagent (Pierce, Rockford, IL). A 20-μg total protein amount was suspended in 1× SDS Sample buffer, heated for 10 min at 70°C, resolved on a 6–12% SDS–PAGE gel (Laemmli, 1970), and transferred to PVDF membrane (Millipore). The blots were blocked in 5% DMP/TBS-T (5% dry milk powder in Tris-buffered saline, 0.01% Tween-20). The blots were incubated for 2 h at room temperature or overnight at 4°C with primary antibody diluted in 1% DMP/TBS-T. The blots were then washed five times for 5 min at room temperature with TBS-T (0.01% Tween-20) and incubated for 1 h at room temperature with horseradish peroxidase–conjugated secondary antibodies (Jackson ImmunoResearch) and washed five times for 5 min at room temperature with TBS-T (0.01% Tween-20), followed by one wash with just TBS. Specific labeling was detected by chemiluminescence reagent (Pierce) with detection using BioMax ML film (Kodak, Rochester, NY). The film was scanned, and the amount of protein was evaluated by densitometry using ImageJ software (National Institutes of Health, Bethesda, MD). The relative band intensity for each protein was obtained through normalization to the intensity of immunoreactive β-actin bands. The statistical significance was calculated using

an unpaired Student's t-test with GraphPad software (GraphPad Software, La Jolla, CA). The final graph was made using Prism software (GraphPad Software).

Immunofluorescence

The Caco2-BBE-Control, Rab25KD, and Rescue cells were plated on 12-well Transwells for 3, 8, and 15 d and then washed with PBS and fixed. For claudin staining, Transwells were fixed with methanol for 5 min at –20°C. For all other staining, the cells were fixed in 4% paraformaldehyde (PFA) for 20 min at room temperature. Cells were washed three times with PBS and then blocked/extracted for 30 min at room temperature in 10% normal goat serum (Jackson ImmunoResearch) and 0.3% Triton X-100 in PBS. Transwells were incubated for 2 h at room temperature or overnight at 4°C with primary antibodies diluted in 1% normal donkey serum and 0.005% Tween-20 in PBS. Transwells were washed three times for 15 min at room temperature with 0.005% Tween-20 in PBS (PBS-T), then incubated for 1 h at room temperature with secondary antibodies diluted as described, washed three times in PBS-T and once in PBS, and then rinsed in water and mounted with ProLong Gold plus 4′,6-diamidino-2-phenylindole (DAPI; Invitrogen).

All images were captured with an Olympus FV1000 confocal microscope (Olympus, Tokyo, Japan) or a Zeiss 510 LSM confocal microscope (Carl Zeiss, Jena, Germany; Vanderbilt Cell Imaging Shared Resource, Nashville, TN) using a 60× oil immersion objective with a numerical aperture of 1.42 and a 5× optical zoom using the microscope's software. The individual images were converted to tif files with the FV1000 or Zeiss LSM software, and then Photoshop (Adobe, San Jose, CA) was used to produce the final figures.

For dual staining of Rab25 with α5-integrin, β1-integrin, and Rab7 using a TSA Kit (PerkinElmer, Waltham MA), the Caco2-BBE cells were plated on 12-well Transwells for 8 d, washed with PBS, and fixed in 4% paraformaldehyde for 20 min at room temperature. Cells were washed three times with PBS and then block/extracted for 30 min at room temperature in 10% normal goat serum (Jackson ImmunoResearch) and 0.3% Triton X-100 in PBS. Transwells were incubated for 2 h at room temperature or overnight at 4°C with primary antibodies diluted in 1% normal donkey serum and 0.005% Tween-20 in PBS. Transwells were washed three times for 15 min at room temperature with 0.005% Tween-20 in PBS-T and then incubated for 1 h at room temperature with secondary antibodies diluted as described and washed three times in PBS-T and once in PBS. The cells were blocked as described and incubated with Rab25 antibody (12C3) overnight at 4°C. The cells were washed five times for 5 min at room temperature with PBS-T, and then cells were incubated with specific secondary antibody conjugated with horseradish peroxidase. The cells washed five times for 5 min. The secondary antibody signal was amplified using cyanine-3 fluorophore–labeled tyramide amplification reagent for 7 min. The Transwells were washed three times for 5 min and rinsed in water and mounted with ProLong Gold plus DAPI (Invitrogen).

All images were captured with an Olympus FV1000 confocal microscope or a Zeiss 510 LSM confocal microscope as described. The colocalization of Rab25 with Rab11a, Rab7, α5-integrin, or β1-integrin was quantitated and analyzed using Imaris Software, version 7.3.1 (Bitplane, Zurich, Switzerland). For each colocalization analysis, 5–10 entire *X-Y* confocal images were analyzed. The threshold values and single time points were selected from two-dimensional scatter plots and histogram modes for both channels. The colocalization matrices were built, and Pearson's *r* and the Manders coefficients were calculated.

PCR quantitation

The Control, Rab25KD, and Rescue cell lines were plated on six-well Transwell filters, and total RNA was extracted using TRIzol reagent according to the manufacturer's instructions. One microgram of RNA was treated with RQ1 RNase-free DNase (Promega, Madison, WI) and used for cDNA synthesis with random hexamers. For RT-PCR, cDNA was made using Advantage 2 RT-PCR kit (Clontech, Mountain View, CA) according to the manufacturer's instructions. Two microliters of five-times-diluted cDNA was amplified using gene-specific primers. β-Actin amplification was used as control to normalize the transcript expression. For quantitative PCR, the cDNA was prepared using High Capacity cDNA Reverse Transcription Kit (Applied Biosystems) with a mix of random and oligo-dT primers according to the manufacturer's instructions. Real-time PCR was performed using a StepOnePlus real-time PCR system with Express SYBR Green ER Supermix (Applied Biosystems) and performed in triplicate for each transcript. The real-time PCR data were analyzed by the comparative C_T method as described by Schmittgen and Livak (2008). The primers were purchased from Sigma Genesys (St. Louis, MO) and validated for melting temperature and efficiency. The primers for the quantitative PCR analysis used were as follows:

Rab25 sense primer: 5′-GACCTCAGCCCTGGACTCTAC-3′

Rab25 antisense primer: 5′-TGATGCAACAGGCCCTCTTCTCC-3′

α5-Integrin sense primer: 5′-TGGAGTCCTCACTGTCCAGC-3′

α5-Integrin antisense primer: 5′-TCGCTCAGTGGCTCCTTCTC-3′

β1-Integrin sense primer: 5′-ATTGGCCTTGCATTACTGCTG-3′

β1-Integrin antisense primer: 5′-AGCTACCTAACTGTGACTATGG-3′

SI sense primer: 5′-TGGCAAGAAAGAAATTTAGTGGA-3′

SI antisense primer: 5′-TTATTCTCACATTGACAGGATC-3′

Villin-1 sense primer: 5′-AAGAAAGCCAATGAGCAGGAGAAG-3′

Villin-1 antisense primer: 5′-TTCTCAATGCGCCACACCTG-3′

Glyceraldehyde 3-phosphate dehydrogenase (GAPDH) sense primer: 5′-AGATCCCTCCAAAATCAAGTGG-3′

GAPDH antisense primer: 5′-GGCAGAGATGATGACCCTTTT-3′

Scanning electron microscopy

A total of 100,000 cells were plated and grown on 12-well Transwells. After 15 d in culture, cells were washed three times with PBS. The cells were fixed with 3% glutaraldehyde in SEM buffer (0.1 M sodium phosphate buffer, pH 7.4, 0.1 M sucrose) at 4°C overnight. Cells were washed with SEM buffer twice, treated with 1% osmium tetroxide (in SEM buffer) on ice for 1 h, and washed three times with SEM buffer. The cells were dehydrated with serial dilutions of ethanol (35, 50, 70, 95, and 100%) for 15 min each and then incubated with hexamethyldisilazane (HMDS). After the HMDS treatment, samples were mounted on stubs and coated with gold in a sputter coater. The cells were analyzed using an FEI Quanta 250 SEM (Vanderbilt Cell Imaging Shared Resource, Vanderbilt University).

Transepithelial resistance measurements

The cell lines were plated on 24-well Transwells, and media were changed every day. The TER was measured using a Millicell-ERS (Millipore) at three different places on each Transwell. The mean was recorded, and the results are expressed in ohm–cm^2.

Soft agar colony growth

A soft agar proliferation assay was performed as described previously (Kuwada and Li, 2000). After 3 wk, the colonies were treated with thiazolyl blue tetrazolium bromide (0.5 mg/ml) for 2 h at 37°C. The colonies were counted using a GelCount colony counter (Vanderbilt Epithelial Biology Center Shared Resource, Vanderbilt University). The results represent the mean of three individual experiments.

Microarray analysis

The Control, Rab25KD, and Rescue cell lines were plated on Transwells for 8 d. On day 8, total RNA was isolated and treated with RNase-free DNase. The RNA from replicate samples was submitted to the Genomics Shared Resource microarray facility at Vanderbilt University. The RNA samples were hybridized to Human Gene 1.0 ST Affymetrix arrays.

Immunoprecipitation

Caco2-BBE Rab25 KD cells transfected with myc-Rab25 were grown for 5 d on Transwells. The cells were washed twice with PBS and lysed with lysis buffer (30 mM Tris-HCl, pH 7.5, 150 mM NaCl, 20 mM Mg acetate, and 1% 3-[(3-cholamidopropyl)dimethylammonio]-1-propanesulfonate [CHAPS]). After 30 min of incubation rotating end over end at 4°C, the lysates were centrifuged at 15,000 × *g* for 15 min at 4°C to remove the cell debris. We precleared 100 µg of lysate protein with 50 µl of Dynabeads for 2 h at 4°C. For immunoprecipitation, the anti-myc antibody, anti–α5-integrin antibody, or nonspecific immunoglobulin G (IgG) was incubated with Dynabeads for 1 h at room temperature. The beads were washed two times with PBS, resuspended in 200 mM triethanolamine (pH 8.2), and incubated for 10 min at room temperature. The beads were cross-linked with 20 mM dimethyl pimelimidate dihydrochloride for 30 min at room temperature. The Dynabeads were washed with 50 mM Tris-HCl (pH 7.5) for 15 min and then three times with TBS. The washed Dynabeads were incubated with precleared lysates overnight. Beads were washed with lysis buffer three times and eluted with 1.5% SDS–PAGE sample buffer and incubation for 10 min at 70°C. The supernatant was analyzed by SDS–PAGE as described.

Cell invasion assay

To assess cell invasion capacity, we used an XCELLigence system (Roche Applied Science, Indianapolis, IN). In a CIM Plate 15, 150 µl of serum-containing media was added to the bottom chamber. The background value was measured in the RTCA DP analyzer. All the cell lines were trypsinized and plated in the top chamber with serum-free media. The CIM plate was left in the culture hood for 10 min, and then it was moved to a 37°C incubator and assembled in the RTCA DP analyzer. The membrane in the CIM plate equilibrated for 1 h. After 1 h, the cell index number was measured every 15 min for 55 h.

Statistical analysis

Descriptive statistics including mean values and SD/SEM were calculated using Excel (Microsoft, Redmond, WA), and *p* values were calculated using an unpaired Student's *t* test with GraphPad software. All data represent at least three independent experiments and are expressed as the mean ± SD/SEM unless otherwise indicated.

ACKNOWLEDGMENTS

Confocal fluorescence imaging was performed through the use of the Vanderbilt University Medical Center Cell Imaging Shared Resource, which is supported by National Institutes of Health Grants CA68485, DK20593, DK58404, and HD15052. This work was supported by National Institutes of Health, National Institute of Diabetes and Digestive and Kidney Diseases Grants RO1 DK048370 and RO1 DK070856 (to J.R.G.). We thank James Higginbotham for assistance with Caco2 cell sorting.

REFERENCES

Boehlke C, Bashkurov M, Buescher A, Krick T, John AK, Nitschke R, Walz G, Kuehn EW (2010). Differential role of Rab proteins in ciliary trafficking: Rab23 regulates smoothened levels. J Cell Sci 123, 1460–1467.

Bretscher MS (1992). Circulating integrins: alpha 5 beta 1, alpha 6 beta 4 and Mac-1, but not alpha 3 beta 1, alpha 4 beta 1 or LFA-1. EMBO J 11, 405–410.

Bryant DM, Datta A, Rodriguez-Fraticelli AE, Peranen J, Martin-Belmonte F, Mostov KE (2010). A molecular network for de novo generation of the apical surface and lumen. Nat Cell Biol 12, 1035–1045.

Buzza MS, Netzel-Arnett S, Shea-Donohue T, Zhao A, Lin CY, List K, Szabo R, Fasano A, Bugge TH, Antalis TM (2010). Membrane-anchored serine protease matriptase regulates epithelial barrier formation and permeability in the intestine. Proc Natl Acad Sci USA 107, 4200–4205.

Casanova JE, Wang X, Kumar R, Bhartur SG, Navarre J, Woodrum JE, Ray GS, Goldenring JR (1999). Rab11a and Rab25 association with the apical recycling system of polarized MDCK cells. Mol Biol Cell 10, 47–61.

Caswell PT, Norman JC (2006). Integrin trafficking and the control of cell migration. Traffic 7, 14–21.

Caswell PT *et al.* (2007). Rab25 associates with alpha5beta1 integrin to promote invasive migration in 3D microenvironments. Dev Cell 13, 496–510.

Cheng JM, Ding M, Aribi A, Shah P, Rao K (2006). Loss of RAB25 expression in breast cancer. Int J Cancer 118, 2957–2964.

Cheng JM, Volk L, Janaki DK, Vyakaranam S, Ran S, Rao KA (2010). Tumor suppressor function of Rab25 in triple-negative breast cancer. Int J Cancer 126, 2799–2812.

Cheng KW, Agarwal R, Mitra S, Lee JS, Carey M, Gray JW, Mills GB (2012). Rab25 increases cellular ATP and glycogen stores protecting cancer cells from bioenergetic stress. EMBO Mol Med 4, 125–141.

Cheng KW *et al.* (2004). The RAB25 small GTPase determines aggressiveness of ovarian and breast cancers. Nat Med 10, 1251–1256.

Dozynkiewicz MA *et al.* (2012). Rab25 and CLIC3 collaborate to promote integrin recycling from late endosomes/lysosomes and drive cancer progression. Dev Cell 22, 131–145.

Ducharme NA, Hales CM, Lapierre LA, Ham AJ, Oztan A, Apodaca G, Goldenring JR (2006). MARK2/EMK1/Par-1Balpha phosphorylation of Rab11-family interacting protein 2 is necessary for the timely establishment of polarity in Madin-Darby canine kidney cells. Mol Biol Cell 17, 3625–3637.

Erickson RP, Larson-Thome K, Valenzuela RK, Whitaker SE, Shub MD (2008). Navajo microvillous inclusion disease is due to a mutation in MYO5B. Am J Med Genet A 146A, 3117–3119.

Goldenring JR, Shen KR, Vaughan HD, Modlin IM (1993). Identification of a small GTP-binding protein, Rab25, expressed in the gastrointestinal mucosa, kidney and lung. J Biol Chem 268, 18419–18422.

Hou J, Gomes AS, Paul DL, Goodenough DA (2006). Study of claudin function by RNA interference. J Biol Chem 281, 36117–36123.

Jones RG, Li X, Gray PD, Kuang J, Clayton F, Samowitz WS, Madison BB, Gumucio DL, Kuwada SK (2006). Conditional deletion of beta1 integrins in the intestinal epithelium causes a loss of Hedgehog expression, intestinal hyperplasia, and early postnatal lethality. J Cell Biol 175, 505–514.

Jung Y *et al.* (2011). Clinical validation of colorectal cancer biomarkers identified from bioinformatics analysis of public expression data. Clin Cancer Res 17, 700–709.

Krishnan M, Singh AB, Smith JJ, Sharma A, Chen X, Eschrich S, Yeatman TJ, Beauchamp RD, Dhawan P (2010). HDAC inhibitors regulate claudin-1 expression in colon cancer cells through modulation of mRNA stability. Oncogene 29, 305–312.

Kuure S, Chi X, Lu B, Costantini F (2010). The transcription factors Etv4 and Etv5 mediate formation of the ureteric bud tip domain during kidney development. Development 137, 1975–1979.

Kuwada SK, Li X (2000). Integrin alpha5/beta1 mediates fibronectin-dependent epithelial cell proliferation through epidermal growth factor receptor activation. Mol Biol Cell 11, 2485–2496.

Laemmli UK (1970). Cleavage of structural proteins during the assembly of the head of bacteriophage T4. Nature 227, 680–685.

Lapierre LA, Avant KM, Caldwell CM, Oztan A, Apodaca G, Knowles BC, Roland JT, Ducharme NA, Goldenring JR (2012).

Phosphorylation of Rab11-FIP2 regulates polarity in MDCK cells. Mol Biol Cell 23, 2302–2318.
Lapierre LA, Caldwell CM, Higginbotham JN, Avant KM, Hall J, Beauchamp RD, Goldenring JR (2011). Transformation of rat intestinal epithelial cells by overexpression of Rab25 is microtubule dependent. Cytoskeleton 68, 97–111.
Lapierre LA, Kumar R, Hales CM, Navarre J, Bhartur SG, Burnette JO, Mercer JA, Bahler M, Goldenring JR (2001). Myosin Vb is associated with and regulates plasma membrane recycling systems. Mol Biol Cell 12, 1843–1857.
Levy P, Robin H, Kornprobst M, Capeau J, Cherqui G (1998). Enterocytic differentiation of the human Caco-2 cell line correlates with alterations in integrin signaling. J Cell Physiol 177, 618–627.
Lobert VH, Brech A, Pedersen NM, Wesche J, Oppelt A, Malerod L, Stenmark H (2010). Ubiquitination of alpha 5 beta 1 integrin controls fibroblast migration through lysosomal degradation of fibronectin-integrin complexes. Dev Cell 19, 148–159.
Marrs JA, Anderson-Fisone C, Jeong MC, Cohen-Gould L, Zurzolo C, Nabi IR, Rodriguez-Boulan E, Nelson WJ (1995). Plasticity in epithelial cell phenotype: modulation by expression of different cadherin cell adhesion molecules. J Cell Biol 129, 507–519.
Mellman I, Nelson WJ (2008). Coordinated protein sorting, targeting and distribution in polarized cells. Nat Rev Mol Cell Biol 9, 833–845.
Muller T *et al*. (2008). MYO5B mutations cause microvillus inclusion disease and disrupt epithelial cell polarity. Nat Genet 40, 1163–1165.
Nam KT *et al*. (2010). Loss of Rab25 promotes the development of intestinal neoplasia in mice and is associated with human colorectal adenocarcinomas. J Clin Invest 120, 840–849.
Pellinen T, Arjonen A, Vuoriluoto K, Kallio K, Fransen JA, Ivaska J (2006). Small GTPase Rab21 regulates cell adhesion and controls endosomal traffic of beta1-integrins. J Cell Biol 173, 767–780.
Pellinen T *et al*. (2008). Integrin trafficking regulated by Rab21 is necessary for cytokinesis. Dev Cell 15, 371–385.
Peterson MD, Mooseker MS (1992). Characterization of the enterocyte-like brush border cytoskeleton of the C2BBe clones of the human intestinal cell line, Caco-2. J Cell Sci 102, Pt 3581–600.
Roberts M, Barry S, Woods A, van der Sluijs P, Norman J (2001). PDGF-regulated rab4-dependent recycling of alphavbeta3 integrin from early endosomes is necessary for cell adhesion and spreading. Curr Biol 11, 1392–1402.
Roland JT, Kenworthy AK, Peranen J, Caplan S, Goldenring JR (2007). Myosin Vb Interacts with Rab8a on a tubular network containing EHD1 and EHD3. Mol Biol Cell 18, 2828–2837.
Roland JTE, Bryant DM, Datta A, Itzen A, Mostov KE, Goldenring JR (2011). Rab GTPase-Myo5B complexes control membrane recycling and epithelial polarization. Proc Natl Acad Sci USA 108, 2789–2794.
Royer C, Lu X (2011). Epithelial cell polarity: a major gatekeeper against cancer. Cell Death Differ 18, 1470–1477.
Schmittgen TD, Livak KJ (2008). Analyzing real-time PCR data by the comparative C(T) method. Nat Protoc 3, 1101–1108.
Schreider C, Peignon G, Thenet S, Chambaz J, Pincon-Raymond M (2002). Integrin-mediated functional polarization of Caco-2 cells through E-cadherin–actin complexes. J Cell Sci 115, 543–552.
Shen L, Weber CR, Turner JR (2008). The tight junction protein complex undergoes rapid and continuous molecular remodeling at steady state. J Cell Biol 181, 683–695.
Shiou SR, Singh AB, Moorthy K, Datta PK, Washington MK, Beauchamp RD, Dhawan P (2007). Smad4 regulates claudin-1 expression in a transforming growth factor-beta-independent manner in colon cancer cells. Cancer Res 67, 1571–1579.
Tzaban S, Massol RH, Yen E, Hamman W, Frank SR, Lapierre LA, Hansen SH, Goldenring JR, Blumberg RS, Lencer WI (2009). The recycling and transcytotic pathways for IgG transport by FcRn are distinct and display an inherent polarity. J Cell Biol 185, 673–684.
Van Itallie CM, Anderson JM (2006). Claudins and epithelial paracellular transport. Annu Rev Physiol 68, 403–429.
Varner JA, Emerson DA, Juliano RL (1995). Integrin alpha 5 beta 1 expression negatively regulates cell growth: reversal by attachment to fibronectin. Mol Biol Cell 6, 725–740.
Vuoriluoto K, Haugen H, Kiviluoto S, Mpindi JP, Nevo J, Gjerdrum C, Tiron C, Lorens JB, Ivaska J (2011). Vimentin regulates EMT induction by Slug and oncogenic H-Ras and migration by governing Axl expression in breast cancer. Oncogene 30, 1436–1448.
Wang E, Brown PS, Aroeti B, Chapin SJ, Mostov KE, Dunn KW (2000). Apical and basolateral endocytic pathways of MDCK cells meet in acidic common endosomes distinct from a nearly neutral apical recycling endosome. Traffic 1, 480–493.